J. Electroanal. Chem, 201 (1986) 329–345
Elsevier Sequoia S.A., Lausanne – Printed in The Netherlands

1,1′-TRIMETHYLENEBISTHYMINE AS SYNTHETIC MODEL OF DINUCLEOTIDE TpT

ELECTROCHEMICAL REDUCTION

TADEUSZ MALINSKI * and JERZY J. LANGER **

Department of Chemistry, Oakland University, Rochester, MI 48063 (U.S.A.)

JACQUES MOIROUX

Lab. Chimie Analitique, U.A. C.N.R.S No. 484, Fac Pharmacie, Université Paris V, 4 Ave. Observatoire, 75270 Paris Cedex 06 (France)

PHILIP J. ELVING ***

Department of Chemistry, University of Michigan, Ann Arbor, MI 48109 (U.S.A.)

(Received 16th July 1985; in revised form 25th November 1985)

ABSTRACT

The electrochemical reduction of 1,1′-trimethylenebisthymine (Thy(C_3)Thy) in dimethylsulfoxide was investigated using dc polarography, cyclic voltammetry, controlled potential electrolysis and spectroelectrochemistry. Thy(C_3)Thy is reduced in a two-electron step ($E_{1/2} = -2.40$ V) to a diradical dianion which abstracts protons from the parent Thy(C_3)Thy to form a neutral free diradical and the Thy(C_3)Thy dianion. The neutral free diradical is further reduced and protonated to form 1,1′-trimethylenebis-dihydrothymine. The dianion forms insoluble mercury salts producing up to three oxidation peaks (E_{pa} between -0.35 and -0.07 V). The effect of added base on the electrochemical and spectroelectrochemical behavior is described. The number of layers of the mercury–Thy(C_3)Thy salt adsorbed in the anodic and stripped in the cathodic processes was calculated. The mechanism of adsorption is discussed.

INTRODUCTION

In order to study interactions of bases bound in nucleic acids in the absence of complicating factors, such as those associated with hydrogen bonding or carbohydrate and phosphodiester linkages, dinucleotide analogs have been synthesized in which the bases are connected by a trimethylene chain: B_1–$(CH_2)_3$–B_2, where B_1 and B_2 are pyrimidine or purine bases. The structure of these analogs is

* To whom correspondence should be addressed.
** Permanent address: Department of Chemistry, A. Mickiewicz University, Poznan, Poland.
*** Deceased.

0022-0728/86/$03.50

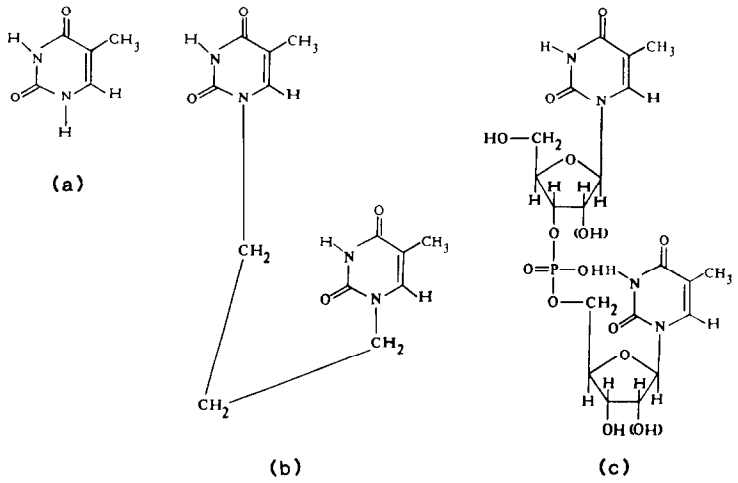

Fig. 1. Formulae for thymine (a), Thy(C_3)Thy (b), and dinucleotide TpT (c).

simpler than those of nucleotides themselves and facilitates evaluation of both photochemical [1–5] and electrochemical [6] results.

Thymine (5-methyl-2,4-pyrimidinedione) (Fig. 1a) is an important constituent of nucleic acids. Of particular interest is the reduction of thymine, because its catabolism proceeds via an initial two-electron transfer by NAD(P)H. Cummings and Elving [7] have investigated the mechanism for the reduction of thymine in dimethylsulfoxide (DMSO) in which the electrochemical behavior of thymine is similar to that of 2-hydroxypyrimidine and uracil, i.e. an initial reduction in a one-electron step to the radical anion. This radical anion reacts with unreduced thymine to produce thymine's conjugate base and, probably, a neutral free radical. The conjugate base forms insoluble mercury salts, which produce oxidation waves between -0.08 and -0.3 V.

Reported here are both electrochemical and spectroelectrochemical studies of 1,1′-trimethylenebisthymine * (Fig. 1b). This compound is a logical bridge for comparing the electrochemistry of thymine and its dinucleotide TpT (thymidyl-3′-5′-thymidine) (Fig. 1c).

EXPERIMENTAL

Chemicals

The procedure for the synthesis of Thy(C_3)Thy has been described previously [1]. This same procedure was used to synthesize 1,1′-trimethylenebishydrothymine.

* The following abbreviation is used in the text: Thy(C_3)Thy. Two thymidine moieties are connected between the 1 and 1′ positions by a methylene bridge. This is in accordance with the suggestion of NAS–NRC Office of Biochemical Nomenclature proposed formally in ref. 8.

Thymine and dihydrothymine (Sigma) were used as substrates for these syntheses. The supporting electrolyte, tetrabutylammonium perchlorate (TBAP) (Eastman Chemical Co. reagent grade) was recrystallized from ethyl acetate, and dried in vacuo prior to use. DMSO (Fisher certified ACS), dried over Linde 4Å molecular sieves, was purified by fractional crystallization, using a method identical to that described for purification of pyridine [9]; the cooling bath was H_2O at 12°C–14°C. Aqueous 25% tetraethylammonium hydroxide (TEAH) solution was obtained from Eastman.

Apparatus

A Princeton Applied Research Model 170 polarograph was used with a jacketed three-compartment cell thermostated at 25°C. Current–voltage curves (potential scan rate up to 0.3 V s^{-1}) and current–time curves were collected on a Houston 2000 X–Y recorder. Rapid cyclic voltammetric data were acquired on a Tektronix 513N oscilloscope with 5A15N and 5A18N plug-ins using a C-5A camera. A platinum button or hanging mercury drop electrode (HMDE), (Metrohm 410 microfeeder) served as the working electrode and a platinum wire as the counter electrode. A saturated calomel electrode (SCE) was used as the reference electrode. For all electrochemical measurements, the SCE was separated from the bulk of solution by a fritted-glass disk. The solution in the bridge consisted only of solvent and supporting electrolyte. This solution was changed periodically to prevent aqueous contamination of the cell solution by the reference electrode. All potentials reported are vs. SCE and have a maximum associated uncertainty of ± 0.005 V.

For controlled electrode potential electrolysis and coulometry, a PAR 174A polarograph and a three-compartment cell were used with a 6 cm^2 mercury pool working electrode.

The spectrophotometric analyses were carried out in-situ in a thin-layer cell which followed the design of Rhodes and Kadish [10]. A mercury–gold minigrid was made from 400 lines/cm gold minigrid (Buckee-Mears Co., St. Paul, MN) by the procedure described previously [11].

The path length of the thin-layer cell was found to be 0.06 cm by both spectrophotometric and electrochemical calibrations. The scan rate for cyclic voltammetry in a thin-layer cell was 0.002 V s^{-1}. Spectrochemical measurements were made with a Tracor Northern 1710 optical spectrometer/multichannel analyzer, which provides time-resolved spectra. Each spectrum results from signal averaging of 100, 5 ms spectral acquisitions; each acquisition represents a single spectrum recorded by a diode-array detector with a resolution of 1.2 nm/channel. Values of λ are accurate to ± 0.5 nm while ϵ is good to $\pm 5\%$ of the absolute value presented.

Procedures

DMSO solutions (0.1 *M* TBAP as background electrolyte) were deoxygenated by purging with purified N_2 for ca. 15 min; a N_2 atmosphere was maintained in the cell throughout the experiment. DME (dropping mercury electrode) data were obtained with a controlled drop-time of 2.0 s, using a capillary with an open-circuit mercury flow rate of 0.91 mg s^{-1}. A new Hg drop (area = 0.0198 cm^2) was used for each

cyclic voltammogram. Coulometric measurements were performed on 12 ml of background and 0.5 mM Thy(C_3)Thy solutions which were stirred continuously using both N_2 and a magnetic stirrer.

RESULTS AND DISCUSSION

Dc polarography and coulometry

A typical dc polarogram for the reduction of 1 mM Thy(C_3)Thy is shown in Fig. 2a. One well-defined reduction is observed at $E_{1/2} = -2.40$ V in DMSO (0.1 M TBAP) solution. The concentration dependence of the Thy(C_3)Thy diffusion current constant, I_d ($I_d = i_l/cm^{2/3}t^{1/6}$), is shown in Fig. 3. The extrapolation of I_d at low c to infinite dilution yields $I_d^\circ = 2.08$. Use of the Matsuda equation [12], which considers shielding effects and best describes the I_d–t behavior at controlled drop times [13], gives a diffusion coefficient, D, of 2.2×10^{-6} which is almost two times lower than that obtained for thymine (see Table 1). The $I_d^\circ = 2.08$ presumably represents a 2 e^- reduction per Thy(C_3)Thy molecule. With this assumption, an I_d of 1.05 for concentrations above 1.2 mM would represent $n = 1.01$ e^-.

Thymine itself has an infinite dilution diffusion current constant, I_d°, of 1.3 which represents a 1 e^- reduction and an I_d of 0.77 above 1 mM which represents

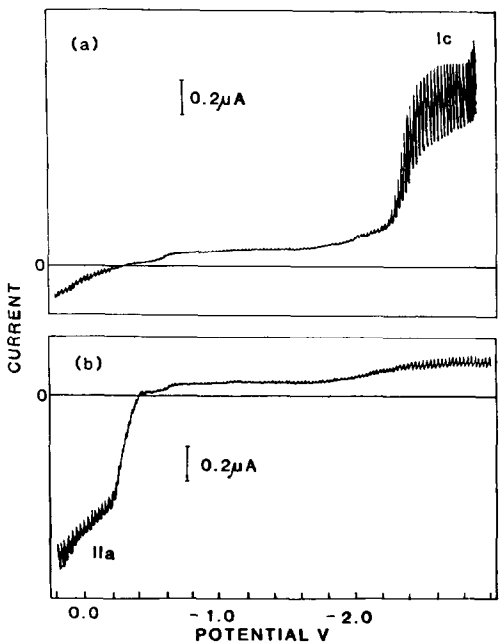

Fig. 2. Dc polarogram of 1 mM Thy(C_3)Thy in DMSO (0.1 M TBAP) solution. (a) Before controlled-potential electrolysis; (b) after controlled-potential electrolysis at −2.60 V.

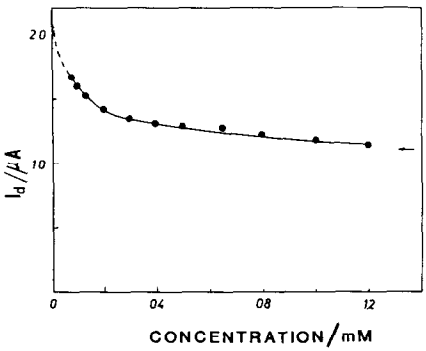

Fig. 3. Concentration dependence of the dc polaragraphic diffusion current constant for Thy(C_3)Thy in DMSO (0.1 *M* TBAP) solution.

an n of 0.59. Therefore, at high concentration of thymine, either about 31% of the radical anion formed during the 1 e^- reduction dimerizes, while 69% is protonated by unreduced thymine, or part of the free radical formed on protonation is reduced in an ECE reaction [7]. The proton transfer, which is probably more rapid than the radical dimerization, deactivates part of the thymine, forming the conjugate base which is more difficult to reduce.

In order to confirm the number of electrons transferred in the reduction step, coulometric measurements were performed in both macro- and microscale electrolysis. For controlled-potential macroscale electrolysis performed at -2.6 V with 12 ml of 0.5 m*M* Thy(C_3)Thy, the charge passed, calculated by planimeter integration of the i–t curve, corresponded to $n = 1.10$, which is similar to that obtained by extrapolation of the I_d–c plot (Fig. 3). Microcoulometric measurement of the reduction of 18 μl of 0.05 m*M* Thy(C_3)Thy in a thin-layer spectroelectrochemical cell yielded a value of $n = 1.7$. Thus, the values of n obtained in microelectrolysis of Thy(C_3)Thy are almost two times higher than that obtained for the reduction of thymine (see Table 1). Both the concentration dependence of I_d and the variation of

TABLE 1

Dc polarographic and cyclic voltammetric [a] data for thymine and Thy(C_3)Thy in DMSO, 0.1 *M* TBAP solution

	$-E_{1/2}$/V [b]	I_d^0/μA s$^{1/2}$ μg$^{-2/3}$ mM^{-1}	n	$10^6 D$/ cm^2 s^{-1}	$-E_p$/V					
					Ic	IIc	IIIc [c]	IIa	IIIa	IVa [d]
Thymine	2.37 (2.36) [e]	1.30 (1.30)	1	4.0 (4.0)	2.44	0.30		0.30	0.20	0.00
Thy(C_3)Thy	2.40	2.08	2	2.2	2.47	0.35	0.29	0.35	0 29	0.07

[a] Scan rate was 0.2 V s^{-1}

[b] Concentration was 1.0 and 0.5 m*M* for thymine and Thy(C_3)Thy respectively.

[c] Measured at scan rate 0.05 V s^{-1}.

[d] Measured at molar ratio TEAH/Thy(C_3)Thy, $r = 1.0$.

[e] Data in parentheses are taken from ref. 7.

n with electrolysis conditions indicate that the Thy (C_3)Thy reduction is not a simple electron transfer, but rather involves coupled chemical reactions with second or higher order kinetics.

Chromatographic analysis of products of the preparative scale electrolysis of Thy(C_3)Thy confirmed the presence of two products of electrochemical reduction (see following discussion). None of the products was found to be a dimer. Therefore, it is reasonable to assume that Thy(C_3)Thy radicals which are formed after the first electron transfer are protonated by unreduced Thy(C_3)Thy and that the protonation step is fast.

A small difference between the half-wave potential of the reduction of thymine and Thy(C_3)Thy was observed (Table 1). A difference in the half-wave potential and electrode mechanism between molecules which contain several electroactive sites (e.g. thymine and Thy(C_3)Thy) can depend upon several factors. These factors are the extent of interactions between the sites, solvation changes, ion pairing, and structural changes of the molecule [14]. For molecules containing identical, noninteracting reaction centers, however, the successive electron transfer will follow simple statistics. In the absence of processes leading to molecular reorganization, the separations between the half-wave potentials will depend only on the number of reaction centers present in a molecule. The difference between the formal potentials E^f for the first and last pair of oxidation states in a molecule of p reaction centers can be described by the following equation [14]

$$E_1^f - E_p^f = (2RT/F) \ln p \tag{1}$$

Therefore, the difference between the E^f for one and two reaction centers should be equal to 35 mV at 25°C.

Figure 4 is a plot of $E_{1/2}$ vs. concentration for thymine and Thy(C_3)Thy, measured under identical experimental conditions. The difference between the $E_{1/2}$ obtained for thymine and that obtained for Thy(C_3)Thy is 35 ± 5 mV in all ranges of concentrations investigated. These results are to be expected because the short

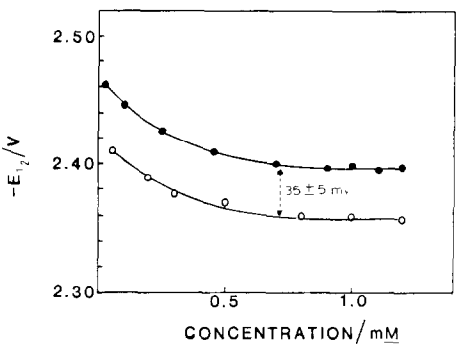

Fig. 4. Concentration dependence of the half-wave potential for thymine (○) and Thy(C_3)Thy (●) in DMSO (0.1 *M* TBAP) solution.

methylene chain in the Thy(C_3)Thy molecule prevents any major interactions between the thymidine moieties in solution. Therefore, each of the thymidine moieties is reduced via an independent one-electron transfer, with no significant differences being observed between the two reductions.

The dc polarogram of the solution obtained after controlled-potential electrolysis at -2.6 V shows an anodic peak at $E_{1/2} = -0.22$ V (see Fig. 2b). The limiting current of this wave is about 80% of that observed in the reduction step. An anodic wave at $E_{1/2} = -0.22$ V was also observed during the titration of Thy(C_3)Thy with TEAH (see following discussion).

Cyclic voltammetry

A cyclic voltammogram of Thy(C_3)Thy in DMSO (0.1 *M* TBAP) is depicted in Fig. 5a. At a HMDE, three processes are observed in the potential range $+0.2$ to -2.7 V. The initial scan shows one cathodic peak at potential, $E_{pc} = -2.47$ V. E_{pc} depends on scan rate with no observable reoxidation peak, and varies linearly with

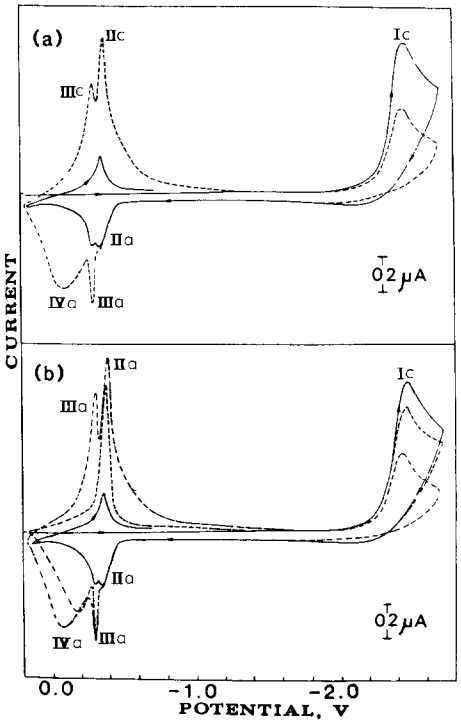

Fig. 5. Cyclic voltammograms of 1 m*M* Thy(C_3)Thy in DMSO (0.1 *M* TBAP) solution at HMDE. (a) Before controlled-potential electrolysis (———) and after electrolysis of 50% of the Thy(C_3)Thy (— — —); (b) effect of added base (TEAH) on the cyclic voltammetric behavior of 1 m*M* Thy(C_3)Thy; molar ratio, *r*, TEAH/Thy(C_3)Thy: 0.0 (———), 0.4 (— — —), and 1.0 (–·–·–).

log v over the scan-rate change of 0.1 to 30 V s^{-1}; however, the slope of the linear relationship is concentration-dependent, ranging from 0.035 V $decade^{-1}$ for 0.2 mM to 0.058 V $decade^{-1}$ at 1.20 mM.

The reverse potential scan shows two distinct anodic peaks at $E_{pa} = -0.35$ and -0.29 V (peak IIa and IIIa in Fig. 5). Because peaks IIa and IIIa were not observed if the switching potential was more positive than the reduction potential of Thy(C_3)Thy, they must be associated with the reduction product of Thy(C_3)Thy.

When the concentration of the reduced form of Thy(C_3)Thy is increased (as during the controlled-potential electrolysis at -2.6 V), no changes of peak IIa are observed; peak IIIa increases to some extent and then remains constant. No changes of peak potentials for either peak IIa or peak IIIa are observed with increasing concentrations of reduced Thy(C_3)Thy. At the concentration where peak IIIa reaches a maximum, a new peak at $E_{pa} = -0.17$ V appears (peak IVa in Fig. 5). Peak IVa is broad, shaped differently from peak IIa and IIIa, and can be shifted to a potential as much as 100 mV more positive when the concentration of the reduced form of Thy(C_3)Thy increases from 10^{-4} to 10^{-3} M.

When the positive scan of potential is reversed at 0.1 V, a new cathodic peak IIc is seen at $E_{pc} = -0.35$ V which is identical to that observed for peak IIa (Table 1). Current of peak IIc increases with concentration of reduced Thy(C_3)Thy to a maximum at about 0.05 mM. At the concentration at which peak IIc current reaches a maximum, a new cathodic peak, IIIc, appears at $E_{pc} = -0.29$ V.

Effect of added base; correlation of electrochemical and spectral behavior

The polarographic and voltammetric behavior of the Thy(C_3)Thy solution titrated with TEAH is equivalent to that of the solution electrolyzed at -2.6 V. (See Figs. 2b and 5.) In cyclic voltammetry, addition of base, TEAH, to 1 mM Thy(C_3)Thy in DMSO (0.1 M TBAP), solution decreases peak Ic and produces peaks IIa, IIIa, and IVa (Fig. 5b; Table 1). Similarly, the dc polarographic wave Ic decreases along with the appearance of an anodic wave at -0.22 V.

A plot of the limiting current and half-wave potential obtained through dc polarography, versus molar ratio, r, of the TEAH/Thy(C_3)Thy solution is given in Fig. 6. A linear extrapolation of the two branches of the curve leads to the point of intersection $r = 0.99$. At molar ratio 2.2, the cathodic wave disappears. The half-wave potential of wave Ic is shifted in a negative direction with increasing r and a similar extrapolation on the plot $E_{1/2} - r$ leads to the point of intersection $r = 1.00$.

Only the protonated forms of Thy(C_3)Thy are reducible within the available potential range. If HT represents the thymine residue, one may expect the following equilibrium in the solutions containing OH^-:

$$HT(C_3)TH \overset{-H^+}{\rightleftharpoons} HT(C_3)T^- \overset{-H^+}{\rightleftharpoons} {}^-T(C_3)T^- \qquad (2)$$

After subtraction of the one proton, the limiting current of wave Ic decreases by about 55% of its original value and a significant shift of the $E_{1/2}$ is observed. This is a consequence of increased negative charge on the molecule, causing the second

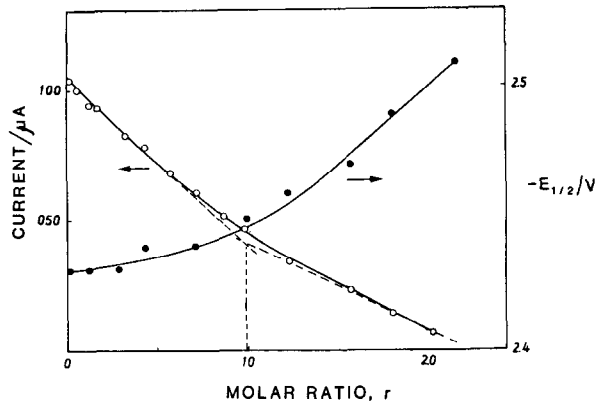

Fig. 6. Dependence of the dc polarographic limiting current (○) and half-wave potential (●) of 0.5 mM Thy(C_3)Thy in DMSO (0.1 M TBAP), on the molar ratio, r, of TEAH/Thy(C_3)Thy.

reduction to be more difficult. The high density of negative charge in the doubly deprotonated form makes further reduction of $^{-}T(C_3)T^{-}$ impossible in the accessible range of potential.

Figure 7 shows the spectra of Thy(C_3)Thy in DMSO at various TEAH concentrations. For 53 μM Thy(C_3)Thy in DMSO (0.1 M TBAP), one peak (peak I) is observed at λ^{I}_{max} 269 nm ($\epsilon^{I}_{max} = 18.8$ mM^{-1} cm^{-1}). Upon addition of TEAH, this 269 nm peak decreases. A second peak (peak II) appears and grows at about $\lambda_{max} = 311$ nm shifting to somewhat shorter wavelengths (up to 306 nm) at increasing r. All curves pass through an isosbestic point at 284 nm which can be attributed to the equilibrium among the protonated and deprotonated species expressed by eqn. (2). In order to correlate the observed spectrophotometric behavior in DMSO solution with the presence of the various forms of Thy(C_3)Thy (i.e. Thy(C_3)Thy

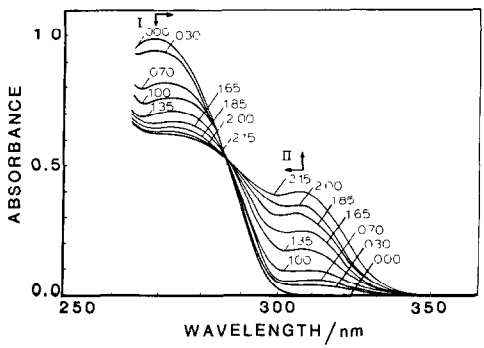

Fig. 7. Ultraviolet absorption of 53 μM Thy(C_3)Thy in DMSO (0.1 M TBAP) at various molar ratios of TEAH/Thy(C_3)Thy (numbers beside curves).

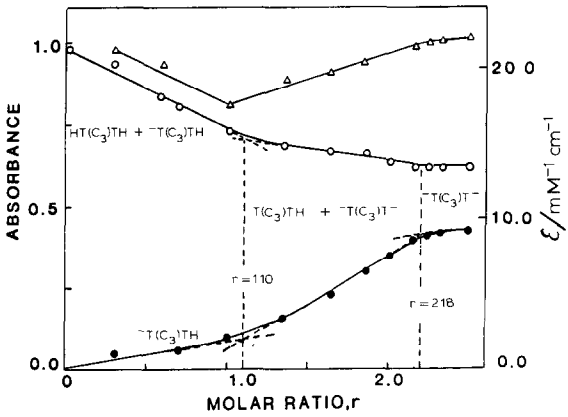

Fig. 8. Dependence of the ultraviolet absorption of $Thy(C_3)Thy$ in DMSO (0.1 *M* TBAP) on the molar ratio, *r*, of TEAH/$Thy(C_3)Thy$. (○) Peak I; (●) peak II; (△) sum of peaks I and II. ϵ is in units of $mM^{-1}\,cm^{-1}$.

itself, the monoanion and dianion), spectrophotometric titration curves were prepared in which peak I and II absorbances were plotted against the molar ratio, *r*, of added TEAH/$Thy(C_3)Thy$ (Fig. 8). The sum of the peak I and II absorbances decreases up to approximately 1.0 *r*, but increases at higher *r* because forms having higher molar absorptivities predominate. In DMSO, $Thy(C_3)Thy$ can exist in both monoanionic ($0 < r < 2.18$) and dianionic ($r > 1.10$) forms. At molar ratios 1.10 and 2.18, all of the 1,1′-trimethylenebisthymine is singly or doubly deprotonated respectively.

Calculated molar absorptivity values of the various forms of $Thy(C_3)Thy$ anions (and also for comparison, thymine anions) are presented in Table 2.

Thin-layer spectroelectrochemistry of 0.12 m*M* $Thy(C_3)Thy$ was done in DMSO (0.5 *M* TBAP) solution. UV spectra were recorded (Fig. 9a) during the voltammetric scan between −1.99 and −2.62 V (Fig. 9b).

During the reduction step, the spectra changed in a way similar to that observed during the spectrophotometric titration with TEAH, i.e. peak I at 269 nm decreases and shifts to a longer wavelength while peak II at 311 nm increases. Unlike the spectrophotometric titration, thin-layer spectra show an additional peak (peak III)

TABLE 2

Ultraviolet spectrophotometric data for thymine [a] and $Thy(C_3)Thy$ species in DMSO (0.1 *M* TBAP) solution

	H_2T	1-HT^-	3-HT^-	T^{2-}	$HT(C_3)TH$	$^-T(C_3)TH$		$^-T(C_3)T^-$	
λ_{max}/nm	266	266	307	305	269	272	311	275	306
$\epsilon_{max}/mM^{-1}\,cm^{-1}$	8.57	7.10	10.80	10.0	18.80	13.20	2.20	11.20	7 80

[a] Data taken from ref. 15.

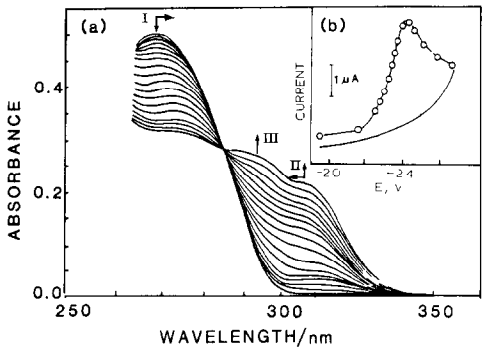

Fig. 9. (a) Thin-layer cyclic voltammogram of 0.5 m*M* Thy(C_3)Thy in DMSO (0.5 *M* TBAP) solution. Scan rate is 2 mV s^{-1}. Open circles indicate potentials where uv-absorption thin-layer spectra were recorded; (b) ultraviolet adsorption, thin-layer spectra of 0.5 m*M* Thy(C_3)Thy in DMSO (0.5 *M* TBAP) solution

at 297 nm. This indicates that the doubly deprotonated Thy(C_3)Thy is not the only product of electrochemical reduction. The peak at 297 nm could be assigned to 1,1′-trimethylenebisdihydrothymine ($H_2T(C_3)TH_2$) (Fig. 12). A synthetic solution made up of 88% Thy(C_3)Thy dianion and 12% 1,1′-trimethylenebisdihydrothymine produced a spectrum identical to that obtained after electrolysis of 0.12 m*M* of Thy(C_3)Thy, confirming the assumptions as to the identity of the products.

Mercury–Thy(C_3)Thy film

Palecek [16] found that pyrimidine bases commonly occurring in nucleic acids form sparingly soluble compounds with mercury which can be stripped cathodically from the mercury electrode.

Attempts have been made to clarify the nature of the mercury thymine film [7], but the precise nature of this film, as well as the process of film formation, are unclear. The mercury–thymine salt presumably involves Hg(I), as does the salt formed with hydroxypyrimidine and uracil anion [17,18]. However, three possible orientations of the thymine anion (one flat and two perpendicular) have to be considered in calculating the electrode area occupied by this anion. The area occupied by thymine ion on the electrode surface for the flat and two possible perpendicular orientations of the thymine ion can be 0.572, 0.306 and 0.277 nm^2 respectively. Therefore, the calculated number of layers of thymine salt deposited on the electrode may vary up to 100% depending upon which orientation is assumed.

Presumably, the Thy(C_3)Thy dianion bonds two Hg(I) cations. Thus, the flat orientation of mercury–Thy(C_3)Thy salt on the surface of mercury is to be expected. This assumed orientation makes a model of adsorption of mercury–Thy(C_3)Thy salt simpler than the model of adsorption of the mercury–thymine salt for which the orientation remains unknown.

Using CPK molecular models [19] to estimate molecular dimensions for a flat orientation, the area occupied by Thy(C_3)Thy dianion on the electrode surface is 0.89 nm^2 which corresponds to a charge density of 35.8 $\mu C\ cm^{-2}$ and electrode surface coverage of 1.86×10^{-10} mol cm^{-2}. On the basis of these results, the number of layers of the mercury–Thy(C_3)Thy salt was calculated using the cyclic voltammetric peak charge method described elsewhere [7]

Peaks IIa and IIIa with a peak separation of only 60 mV show some overlapping. However, the ability to control finely the appearance of peaks by concentration of Thy(C_3)Thy dianion IIa and IIIa, as well as their sharpness and symmetry permit confidence in the following charge calculations. The concentration of Thy(C_3)Thy anion was maintained at the proper level by addition of doubly deprotonated Thy(C_3)Thy to DMSO (0.1 *M* TBAP, 10^{-4} *M* TEAH) solution used in the cyclic voltammetric measurement of film deposition. This was necessary to avoid the influence of additional amounts of one of the products of reduction Ic, Thy(C_3)Thy dianion, whose concentration is changed depending on the conditions of the electrochemical experiment. Therefore, voltammograms used for charge calculations were recorded from a starting potential of -1.6 V with a switching potential of $+0.1$ V.

The number of layers deposited and stripped versus concentration of Thy(C_3)Thy anion is plotted in Fig. 10a. In the absence of Thy(C_3)Thy anion no peaks were observed in the potential range -1.6 to $+0.1$ V. At concentrations up to 8×10^{-6} *M*, only the first anodic peak IIa was observed. The charge under this peak, calculated at 8×10^{-6} *M*, is $33.0 \pm 0.5\ \mu C\ cm^{-2}$ which indicates that about 93% of the mercury surface is covered by a monolayer of mercury–Thy(C_3)Thy salt. At a concentration higher than 8×10^{-6} *M*, a peak IIIa started to appear. The charge under this peak increases linearly and reaches a maximum ($32.0 \pm 0.5\ \mu C\ cm^{-2}$) at concentration 1.5×10^{-5} *M* which corresponds to the second monolayer coverage. No further changes of charge under peak IIIa or peak IIa are noted at concentrations above 1.5×10^{-5} *M*. At 1.6×10^{-5} *M*, peak IVa appeared and the number of layers deposited under this process increases from about one (at 2.0×10^{-5} *M*) to about eleven (at 1.1×10^{-4} *M*). Further addition of up to 15% of dihydrothymine to Thy(C_3)Thy solution with TEAH did not have any significant influence on the adsorption of Thy(C_3)Thy anions.

The number of layers of mercury–Thy(C_3)Thy salt stripped (q_s) under cathodic peak IIc is identical to that deposited (q_d) under processes IIa and IIIa only for $q_d = 2$ (Fig. 10b). At concentrations of Thy(C_3)Thy dianion higher than 2.5×10^{-5} *M*, q_d is higher than q_s. The deposition of more than two layers of salt may result in the loss of a portion of subsequent layers through non-adherence to the electrode surface. This effect would be expected to increase with both the amount of film deposited and the time from deposition to stripping. The observed results show both dependencies. A similar effect has been observed for the mercury–thymine salt [7].

On the basis of the cyclic voltammetric, titrimetric and coulometric data, the overall mechanism of mercury–Thy(C_3)Thy salt adsorption and film formation is proposed as shown schematically in Fig. 11. The dianion of Thy(C_3)Thy formed

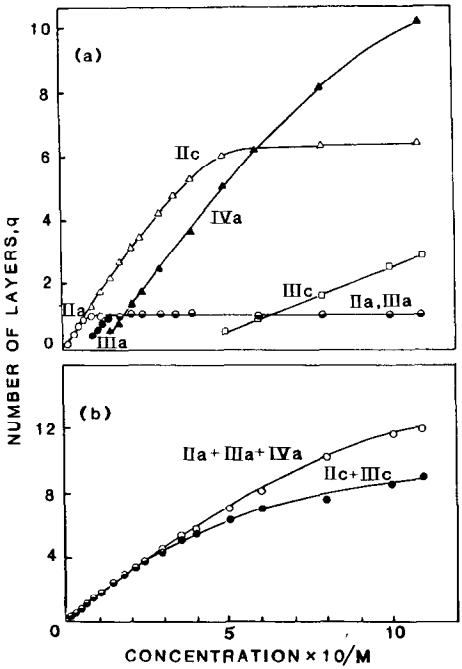

Fig. 10 (a) Number of layers of mercury–Thy(C_3)Thy salt deposited [peak IIa (○), IIIa (●), IVa (▲)], and stripped from the electrode surface [peak IIc (△) and IIIc (□)] versus concentration of Thy(C_3)Thy dianion. (b) Total number of layers of mercury–Thy(C_3)Thy salt deposited and stripped; anodic processes (○) and cathodic processes (●).

during the first reduction at $E_{pc} = -2.47$ V in a reverse potential scan reacts with Hg(I) generated at -0.35 V.

$$2\,Hg + {}^{-}T(C_3)T^{-} - 2\,e^{-} \rightleftharpoons HgT(C_3)THg \qquad (3)$$

This salt of Hg(I)–Thy(C_3)Thy forms a monolayer, strongly bonded to the mercury

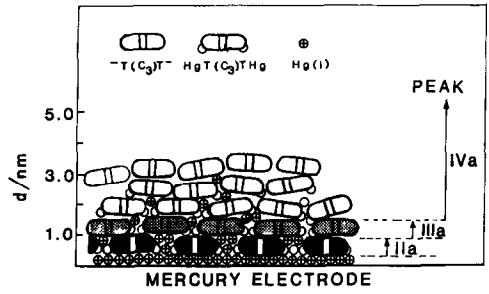

Fig. 11 Model for adsorption of Thy(C_3)Thy anions on mercury electrode; long segments represents thymine anion; (black and dotted: strong adsorption). Roman numerals indicate peaks obtained in cyclic voltammetry

surface. About 90% of the mercury surface is blocked by the adsorbed layer, which causes diffusion of Hg(I) cations from the electrode to the bulk solution to be more difficult, but possible. The diffusion of Hg(I) is the slowest step among the two other steps involved in the kinetics of reaction (3), i.e. electrogeneration of Hg(I) and diffusion of Thy(C_3)Thy anions from the bulk solution to the electrode surface. If the potential scan rate is faster than 0.3 V s^{-1}, peak IIIa decreases significantly. This decrease occurs because the potential for the formation of the second layer is reached faster than the time needed for a significant amount of Hg(I) to diffuse through the first layer. At slow potential scan rates ($v < 0.3$ V s^{-1}), the second monolayer of Hg(I)–Thy(C_3)Thy salt is formed. After formation of the second monolayer, the structure of the film of subsequent layers of Thy(C_3)Thy–mercury salt deposited is different due to the, now impeded, slow diffusion of the mercury cations through the closely packed film of the first two layers. This slow diffusion determines the kinetics of salt formation and affects the adsorption process and structure of the deposited film. The overall effect can be seen in cyclic voltammetry as a broadening of peak IVa (see Fig. 5). The width of peak IVa increases significantly with potential scan rate. Also, the cohesive forces between later salt layers are not as strong as in the case of the first two layers and a partial film loss, probably due to mechanical detachment preceding or during film reduction, is observed (Fig. 10b).

Stripping of the adsorbed layers occurs for $q_d \leqslant 6$, at -0.35 V (peak IIc) which is exactly the same potential observed for deposition under anodic process IIa. This is fairly strong evidence that the observed faradaic process involves a film formation. The stripping involves reduction of Hg(I) to metallic mercury and diffusion of Thy(C_3)Thy anions from the reaction layer to the bulk solution. For $q_d > 6$, diffusion of the Thy(C_3)Thy anions from the electrode surface is probably more difficult; a second stripping process (peak IIIc) appears at a potential which is identical to that observed for deposition process IIIa. This indicates that the stripping process IIIc occurs after reduction of molecules from the second layer. The reduction under process IIIc is easier than reduction under process IIc and occurs until the total number of layers is reduced to six (Fig. 10a).

Presented data are consistent with those obtained for thymine and also for uracil and 2-hydroxypyrimidine [7,17,18]. Information obtained for Thy(C_3)Thy does not support a thesis that oxidation peak IIa and IIIa, also observed for thymine, can be due to the formation of two different mercury–thymine salts. While thymine anion exists as a mixture of deprotonated forms at N(1) and N(3) (Fig. 1) and since the mercury salts of these two anionic forms may have different solubilities, two deposition peaks may be expected. However, Thy(C_3)Thy which is deprotonated only at N(3) and forms only one salt also exhibits peaks IIa and IIIa. Therefore, it follows that the appearance of two peaks observed for thymine cannot be due to the formation of two different salts.

Mechanism

On the basis of both electrochemical and spectroelectrochemical data as well as studies of similar compounds [7,18,20], a summary of the mechanism for the

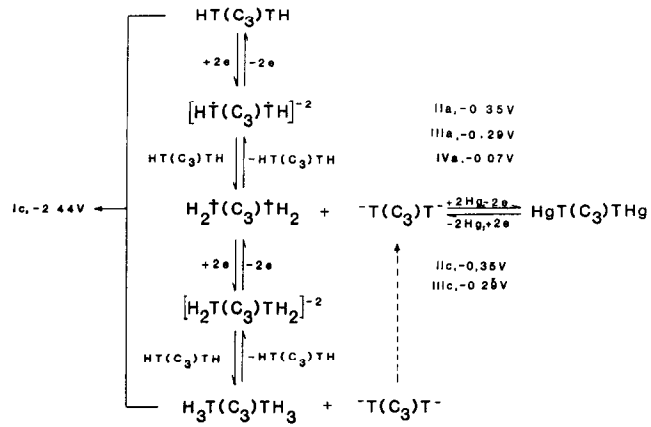

Fig. 12. Reduction mechanism for 1,1′-trimethylenebisthymine in DMSO. Symbols: Thy(C_3)Thy = HT(C_3)TH, 1,1′-trimethylenebisthymine; [HṪ(C_3)ṪH]$^{-2}$, diradical dianion; H_2Ṫ(C_3)ṪH_2, free diradical; [H_2T(C_3)TH_2]$^{-2}$, reduced free radical; H_3T(C_3)TH_3, 1,1′-trimethylenebisdihydrothymine; Roman numerals are peak designations (ref. Fig. 5).

reduction of Thy(C_3)Thy can be considered as shown in Fig. 12. This mechanism is consistent with that proposed for the reduction of thymine.

Thy(C_3)Thy is reduced in a 2 e^- step and forms the diradical dianion. The diradical dianion undergoes a rapid protonation by the parent compound. Such a proton transfer has been observed for thymine, 2-hydroxypyrimidine, and uracil [7,17,18]. This transfer deactivates part of the Thy(C_3)Thy, which would otherwise be available for reduction and forms Thy(C_3)Thy anion, which is more difficult to reduce. Thy(C_3)Thy anion forms an insoluble mercury salt. The free radical which is also a product of the deprotonation step is reduced in a subsequent two-electron transfer. This step was not observed for uracil or 2-hydroxypyrimidine. Products of this reaction are 1,1′-trimethylenebisdihydrothymine and Thy(C_3)Thy anion.

During these studies, attempts were made to find an ESR signal due to presence of Thy(C_3)Thy diradical dianion by electrolyzing the solution of Thy(C_3)Thy at -2.6 V in the ESR cavity and freezing the electrolyzed solution in liquid nitrogen. These attempts were unsuccessful, probably due to fast protonation of the Thy(C_3)Thy diradical dianion by unreduced Thy(C_3)Thy, resulting in a free diradical and a dianion. Because this free diradical can be reduced easily by the parent compound, the free diradical is probably also a short-lived species. Thymine anion radical has been produced, and its ESR spectrum obtained during photolysis of thymine in an alkaline glass at 77 K [21]. Under these conditions, the radical, which was stable for as little as 15 s, produced a dark blue color in glass. The radical yield is much higher in flash photolysis than during electrolysis. Consequently, the concentration of unreduced species is small and protonation by the parent compound is negligible in photolysis. Both effects as well as the time scale of photolysis and electrochemical experiments play significant roles in the detection of the anion radical.

The presence of Thy(C_3)Thy dianion and 1,1′-trimethylenebishydrothymine was detected by thin-layer, UV–visible spectroelectrochemistry, and the compounds were separated by liquid chromatography and characterized. The product solutions from electrolysis were freeze-dried and redissolved in a small volume of DMSO and passed through a column of Sephadex LH-20 using DMSO as the eluent. Two peaks were obtained in LC at retention volumes of 150 (peak I) and 220 ml (peak II). Peak II was observed also for the product obtained after the titration of Thy(C_3)Thy with TEAH. Therefore, the peak at a retention volume of 220 ml can be assigned to Thy(C_3)Thy anion or salt. The 1,1′-trimethylenebisdihydrothymine produced a peak at the retention volume 150 ml. Additional confirmation that the compound in peak II is 1,1′-trimethylenebisdihydrothymine came from comparison of IR spectra for the electrochemically generated product, separated under peak I and synthetic 1,1′-trimethylenebisdihydrothymine.

An additional goal of chromatographic separation was to find out whether any dimer is produced during electrochemical reduction of Thy(C_3)Thy. Certainly, intermolecular and intramolecular dimerization of the diradical produced during the reduction step is possible. On the basis of studies of similar compounds [20] the rate constant of intermolecular dimerization of RH_2 may be expected to be of the order of 10^6 to 10^8 M^{-1} s^{-1}. Previous studies have shown that acetone-sensitized photolysis at 300 nm of Thy(C_3)Thy has yielded, through stereochemical control of intramolecular dimerizatiion, *cis–syn*, *trans–anti*, and *cis–anti* cyclobutane-type products [2]. However, there is no peak on the chromatogram which could be assigned to the dimer. It has been suggested that the thymine dimerization is much slower than that of uracil [7]. The 5-methyl group on thymine would hinder dimerization sterically if the dimerization were to occur at C(4), C(5) or C(6). The steric effect is expected to be more significant in the case of Thy(C_3)Thy diradical intermolecular dimerization. We also cannot exclude that any intermolecular dimer formed undergoes decomposition during chromatographic separation.

In conclusion, we have presented an electrochemical characterization of Thy(C_3)Thy, a synthetic analogue of dinucleotide TpT. In addition to obtaining new spectral data for the dianion of Thy(C_3)Thy, we have also generated electrochemical spectra for 1,1′-trimethylenebisdihydrothymine.

Although the mechanism for the reduction of Thy(C_3)Thy and thymine are similar, it must be noted that a clearer interpretation of film formation was obtained in the case of Thy(C_3)Thy.

ACKNOWLEDGEMENTS

We acknowledge the assistance of J. Bennett and J. Fish. This work was supported by BRSG Grant S07RR7131.

REFERENCES

1 D.T. Brown, J. Eisinger and N.J. Leonard, J. Am. Chem. Soc., 90 (1968) 7302.
2 N.J. Leonard, K. Golankiewicz, R.S. McCredie, S.M. Johnson and J.C. Paul, J. Am. Chem. Soc., 91 (1969) 5855.
3 N.J. Leonard and R.L. Cundall, J. Am. Chem. Soc., 96 (1974) 5904.
4 K. Golankiewicz and L. Strekowski, Mol. Photochem., 4 (1972) 189.
5 K. Golankiewicz and F. Kazmierczak, Mol. Photochem., 7 (1976) 181.
6 J.J Langer and T. Malinski, Bioelectrochem. Bioenerg., 8 (1981) 7.
7 T.E. Cummings and P.J. Elving, J. Electroanal. Chem., 102 (1979) 237.
8 W.E. Cohn, N.J. Leonard and S.V. Wang, Photochem. Photobiol., 19 (1974) 89.
9 D.A. Hall and P.J. Elving, Anal. Chim. Acta, 39 (1967) 141.
10 R.K. Rhodes and K M. Kadish, Anal. Chem., 53 (1981) 1539.
11 M.L. Meyer, T.P. DeAngelis and W.R. Heineman, Anal. Chem., 49 (1977) 602.
12 H. Matsuda, Bull. Chem. Soc. Jpn., 26 (1953) 342.
13 T.E. Cummings and P.J. Elving, Anal. Chem., 50 (1978) 480.
14 J.B. Flanagan, S. Margel, A.J Bard and F.C. Anson, J. Am. Chem. Soc., 100 (1978) 4248.
15 T. Malinski, W.T. Bresnahan, T.E. Cummings and P.J. Elving, Bull Soc. Chim. Fr., (1980) I–410.
16 E. Palecek, Anal. Biochem., 108 (1980) 129.
17 T. Wasa and P.J. Elving, J. Electroanal. Chem , 91 (1978) 249.
18 T.E. Cummings and P.J. Elving, J. Electroanal. Chem., 94 (1978) 123.
19 CPK Precision Molecular Models, The Ealing Corporation, 2225 Massachusetts Avenue, Cambridge, MA 02140.
20 P.J Elving in G. Milazzo (Ed.), Topics in Bioelectrochemistry and Bioenergetics, Vol. 1, Wiley, London, 1976, pp. 179–286.
21 M.D Sevilla, J. Phys. Chem., 745 (1971) 626.